



Study on structure and properties of tubular braid-reinforced poly(lactic acid) (PLA) hollow fiber membranes

Chuanmin Xiao^a, Changfa Xiao^{a,*}, Mingxing Chen^b, Heng Huang^a

^aState Key Laboratory of Separation Membranes and Membrane Processes, School of Material Science and Engineering, Tianjin Polytechnic University, No. 399 Binshui West Road, Tianjin, 300387, China, Tel. +86 022-83955299; emails: xiaochangfa@163.com (C. Xiao), 316098186@qq.com (C. Xiao), 1129786453@qq.com (H. Huang)

^bSchool of Textile and Garments, Hebei University of Science and Technology, No.26, Yuxiang District, Shijiazhuang, 050018, China, email: 838144595@qq.com

Received 13 November 2018; Accepted 13 April 2019

ABSTRACT

The tubular braid-reinforced (BR) poly(lactic acid) (PLA) hollow fiber membranes were prepared by concentric circular spinning technology in this study. The effect of polyethylene glycol (PEG) molecular weight on the structure and properties of the homogenous-reinforced (HMR) PLA hollow fiber membranes was investigated. Besides, the effect of tubular braid materials on the interfacial bonding performance was also studied. The results showed that with the increase of PEG molecular weight, the mean pore size showed a decreasing trend and the membrane surface became rougher which induced the hydrophilicity to increase. In addition, the water flux of the membranes increased first and then decreased. While, the BSA rejection and the anti-fouling performance increased with the increase of PEG molecular weight. When the PEG molecular weight was 10,000, obtained membranes exhibited a high pure water flux of 135.8 L m⁻²h⁻¹ and BSA rejection of 96.1%. It was also found that the interfacial adhesion of HMR PLA hollow fiber membranes was better than that of the heterogeneous-reinforced (HTR) PLA hollow fiber membranes.

Keywords: Poly(lactic acid); Polyethylene glycol; Tubular braid-reinforced; Hollow fiber membranes; Interfacial bonding

1. Introduction

In recent years, porous membranes such as micro-filtration (MF) and ultrafiltration (UF) membranes have been widely applied in the treatment of various industrial wastewater, municipal sewage and domestic sewage [1,2]. The membrane bioreactor (MBR) has been widely applied for water reclamation due to the combination of activated sludge processes with membrane separation processes [3]. Mechanical properties of hollow fiber membranes were very important during the process of MBR. While the mechanical properties of the hollow fiber membranes prepared via the traditional non-solvent induced phase separation (NIPS)

method were relatively poor [4–6], a relatively simple and efficient method to enhance the mechanical properties of hollow fiber membranes was coating a separation layer on a high-strength matrix. Zenon Environmental Inc. [7] and Kolon Industries, Inc. [8] developed the reinforced membranes comprising the tubular braid as the reinforcement and the layer of polymeric membrane coated on the outer surface of tubular braid. However, the separation layer of such a hollow fiber membrane was extremely easy to peel off from the tubular braid as the separation layer was thermodynamically incompatible with the tubular braid [9]. Due to some special circumstances during the separation process and the cleaning process of the membranes after use, it was

* Corresponding author.

desirable to develop a hollow fiber membrane with higher interfacial bonding between the separation layer and the tubular braid [10].

Our research team has made a lot of researches on the preparation of reinforced hollow fiber membranes. Zhang et al. [9] prepared the HMR and heterogeneous-reinforced (HTR) hollow fiber membranes with polyvinylidene fluoride (PVDF) and polyacrylonitrile (PAN) as the separation layer, respectively, wherein the PVDF hollow fiber membranes which were prepared via melt spinning method were applied as the reinforcement. Liu et al. [11,12] also prepared the HMR and HTR hollow fiber membranes with polyvinylchloride (PVC) and PVDF as the separation layer, respectively, wherein the PVC hollow fiber membranes which were prepared via melt spinning method were applied as the reinforcement. They found that the HMR hollow fiber membranes showed excellent interfacial bonding state than the HTR hollow fiber membranes. Fan et al. [13] prepared the tubular-braid reinforced (BR) cellulose acetate (CA) hollow fiber membranes, wherein the CA, PAN and their 'hybrid' tubular braid were applied as the reinforcement, respectively. The result showed that the best ratio of the fibers in the tubular braid was 2/1 (CA/PAN) taking into account both interfacial bonding state and membrane permeability. Therefore, the materials of reinforcement have an important effect on the properties of reinforced hollow fiber membranes.

At present, most porous membranes are made from a variety of polymers extracted from petrochemicals [14–18], which can cause waste of resources and environmental pollution. Therefore, the source of membrane materials has begun to receive widespread attention in recent years. Currently, the biopolymers such as PLA, polyhydroxyalkanoates (PHA), poly(butylene succinate) (PBS), etc., have great potential for application in the field of membrane technology due to their biodegradability, low toxicity and good biocompatibility [19]. As one of the most investigated and commercially used biopolymers, PLA was formed by polymerization of lactic acid monomers, which can be produced from agricultural products and by-products. Therefore, the application of PLA can reduce the emission of CO₂ and other derivatives generated from petroleum materials. Moreover, PLA was biodegradable and environmentally friendly [20–22].

As an environmentally friendly material, PLA has been already used in membrane technology for different applications [23,24], such as water treatment, pervaporation, gas separation, etc. Moriya et al. [25] prepared PLA hollow fiber membranes for water treatment, the result showed that the PLA hollow fiber membranes showed high water permeability and separation performance. Minbu et al. [26] prepared PLA membranes with Tween 80 as a surfactant for water treatment, the result showed that the PLA membrane with 10 wt.% Tween 80 showed high retention of bacterial cells and a high permeability of protein molecules. Abdellatif et al. [27] developed a new method for PLA grafting onto CA for high performance bio-based membranes for ethyl tert-butyl ether (ETBE) purification, the result showed that the PLA grafted onto CA strongly improved the flux ($\times 12$) while the ethanol permeate content remained in the very high range ($C' > 90$ wt.%) for ETBE purification by pervaporation. Zereshki et al. [28] prepared PLA membranes with poly

(vinyl pyrrolidone) (PVP) as the additive for the pervaporative of ethanol/cyclohexane (EtOH/CH_x) azeotropic mixture, the result showed that all the membranes were EtOH selective and the highest separation factor reached up to 120 when the PVP concentration was 11 wt.%. Komatsuka and Nagai [29] prepared PLA membranes for gas separation, the result showed that gas permeability and permselectivity of PLA membranes were not significantly affected by a change in chain mobility at glass transition. Iulianelli et al. [30] prepared PLA membranes for gas separation, the result showed that the Robeson's upper-bound [31] had been overcome, achieving an ideal selectivity H₂/CO₂ around 25 with an H₂ permeability of 25 barrer.

PLA membranes were mostly prepared by NIPS or thermal-induced phase separation (TIPS) in previous study [32–34]. However, there were some drawbacks of the membranes which were prepared by NIPS and TIPS. The membranes prepared by NIPS method had high precision of separation, while its mechanical properties were poor due to its large finger-like pore structure [26]. The TIPS method was easy to obtain the membrane with high strength, while separation accuracy was low [35]. Until now, there were no studies which focused on the preparation of PLA hollow fiber membranes with high strength and high separation accuracy have been reported. Therefore, it was valuable to prepare PLA hollow fiber membranes with high strength and separation accuracy.

In this paper, the BR PLA hollow fiber membranes were prepared with tubular braid as the reinforcement and PLA as the membrane-forming polymer. First, the effect of PEG molecular weight on the structure and properties of the HMR PLA hollow fiber membranes was investigated. Second, the HMR and HTR PLA hollow fiber membranes were prepared, and the interfacial bonding properties between the separation layer and the reinforcement were studied.

2. Experimental

2.1. Materials

Poly(lactic acid) (PLA 4032D) was purchased from Nature works (USA). Polyethylene glycol (PEG, Mw = 400; 2,000; 10,000; 20,000) and N-methylpyrrolidone (NMP, >99.5%) were obtained from Tianjin Kermel Chemical Reagent Co., Ltd. (Tianjin, China). PLA and PET filaments were supplied by Zhejiang Xuri Fiber Co., Ltd. (Zhejiang, China) and Sinopec Yizheng Chemical Fibre (Yizheng, China), respectively. Bovine serum albumin (BSA, Mw = 68,000) were purchased from Beijing Solarbio Science & Technology Co., Ltd. (Beijing, China).

2.2. Preparation of BR PLA hollow fiber membranes

The BR PLA hollow fiber membranes were fabricated via concentric circular spinning technology according to previous study [13]. Before this process the tubular braid was prepared by the two-dimensional braided technology with PLA or PET filaments. Fig. 1 shows the apparatus of concentric circular spinning technology. A specified amount of PLA, PEG and NMP were added in to a three-necked round-bottom flask and the mixtures were vigorously stirred for

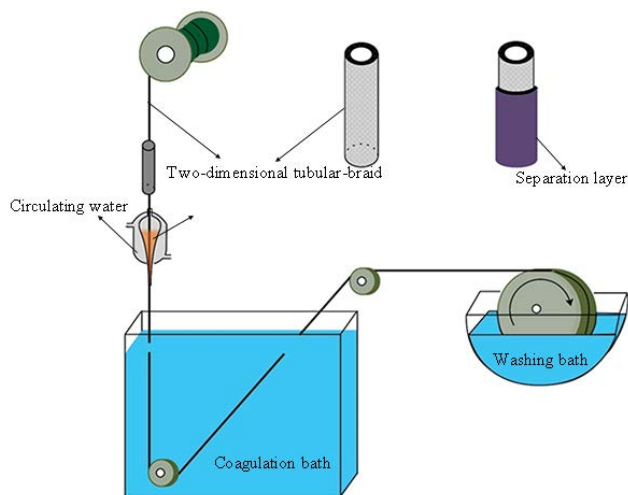


Fig. 1. Schematic diagram of concentric circular spinning technology.

5 h at 80°C to obtain homogeneous casting solution. Then, the obtained membranes were immersed in deionized water for 48 h to wash out residual solvent and water-soluble additive. The spinning parameters of PLA hollow fiber membranes with different casting solutions are shown in Table 1.

2.3. Characterization of the BR PLA hollow fiber membranes

2.3.1. Casting solution viscosity

The shear viscosity of casting solutions was measured using a rotary rheometer (HAAKE MARS, Thermo Fisher Scientific, USA) at test temperature of 80°C. Shear stress was measured over a range of shear rate from 0 to 500 s⁻¹.

2.3.2. Morphology

The morphology and surface roughness of the BR PLA hollow fiber membranes were observed using a scanning electron microscope (SEM), (S4800, HITACHI, Japan) and

atomic force microscope (AFM), (S5500, Agilent, USA). The membranes were lyophilized, followed by fracturing to expose their cross-sectional areas and surface. Thereafter, they were sputtered with gold before SEM analysis.

2.3.3. Water contact angle

The water contact angle of BR PLA hollow fiber membranes was measured by an optical contact angle measuring instrument (DSA100, KRUSS, Germany).

2.3.4. Pore size distribution

The pore size distribution of the BR PLA hollow fiber membranes was tested using a bubble point filter aperture meter (3H-2000PB, Beijing Beishide Instrument Technology, China).

2.3.5. Tensile strength

The tensile strength of the BR PLA hollow fiber membranes was determined at room temperature by an electro mechanical testing machine (JBDL-200N, Yangzhou Jingbo, China). The gripping range and tensile rate were set at 100 mm and 100 mm min⁻¹, respectively.

2.3.6. Bursting strength

The pressure at which the separation layer break was defined as the bursting strength of the BR PLA hollow fiber membranes. The bursting strength was tested by physical washing using a water flux meter through an internal pressure method, and pressurized at a rate of 0.001 MPa min⁻¹.

2.3.7. Ultrasonic water bath oscillation determination

The BR PLA hollow fiber membranes were ultrasonically oscillated by an ultrasonic cleaning machine (US-22D, Beijing Kezhen Century Technology, China). The ultrasonic wave power was 360 W, ultrasonic frequency was 40 kHz. The pure water flux (PWF) and BSA rejection of the sonicated membranes were tested.

Table 1
Spinning parameters of PLA membranes with different casting solution composition

Membrane	PLA (wt.%)	PEG molecular weight (Da)	PEG (wt.%)	NMP (wt.%)	Tubular braid
M0	18	–	–	82	PLA
M1	18	400	5	77	PLA
M2	18	2,000	5	77	PLA
M3	18	10,000	5	77	PLA
M4	18	20,000	5	77	PLA
M5	18	10,000	5	77	PET
Spinning temperature (°C)	80				
Extra coagulation water (°C)	25				
Air gap (cm)	10				
Take up speed (m h ⁻¹)	30				

2.3.8. Permeation

The PWF of BR PLA hollow fiber membranes was measured by a laboratory-made water flux meter (Fig. 2) at 0.1 MPa. The PWF was calculated by the following equation:

$$J = \frac{V}{A \times t} \quad (1)$$

where J is the PWF ($\text{L m}^{-2} \text{h}^{-1}$), A is the effective area of the membranes (m^2), t is the test time (h), V is the quantity of the permeate (L).

The protein solution permeate flux (PSF) of the BR PLA hollow fiber membranes was measured with 1 g L^{-1} BSA aqueous solution at 0.1 MPa and calculated by Eq. (1). The concentration of feed solution and permeate solution was determined by UV spectroscopy (UV-1810, Purkinje General, China) at a wavelength of 280 nm. The BSA rejection was calculated by the following equation:

$$R = \left(1 - \frac{C_p}{C_f} \right) \times 100\% \quad (2)$$

where R is the rejection, and C_f and C_p are the concentrations of feed and permeate solution (g L^{-1}), respectively.

2.3.9. Anti-fouling performance

The anti-fouling performance of BR PLA hollow fiber membranes was characterized by flux recovery ratio (FRR) and flux decline ratio (DR), which can be calculated by the following equations:

$$\text{FRR} = \left(\frac{J_2}{J_0} \right) \times 100\% \quad (3)$$

$$\text{DR} = \left(\frac{J_0 - J_1}{J_0} \right) \times 100\% \quad (4)$$

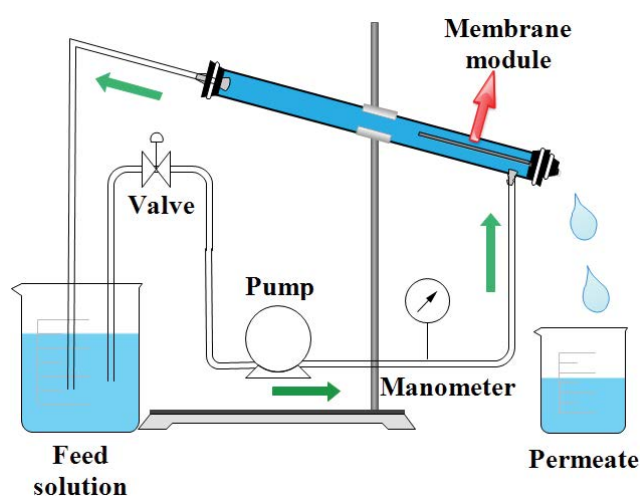


Fig. 2. Pure water flux meter device schematic.

where J_0 is the original PWF ($\text{L m}^{-2} \text{h}^{-1}$), J_1 is the protein solution permeate flux ($\text{L m}^{-2} \text{h}^{-1}$), J_2 is the recovery flux ($\text{L m}^{-2} \text{h}^{-1}$).

3. Results and discussion

3.1. Effect of PEG molecular weight on HMR PLA hollow fiber membranes

Fig. 3 shows the shear viscosity of the casting solutions with different PEG molecular weight. As can be seen from the figure, the shear viscosity of the casting solution increased with the increase of the PEG molecular weight. Due to PEG solubility in the NMP decreased with the PEG molecular weight increase [36,37], the higher molecular weight of PEG, the molecular chains were easier to entangle with the PLA molecular chains. Hence, the movement of segments was blocked and flow resistance increased which induced the shear viscosity to increase.

Fig. 4 shows the SEM and AFM images of the HMR PLA hollow fiber membranes with different PEG molecular weight. It can be seen clearly that the interfacial bonding between the separation layer and PLA tubular braid was well. The casting solution can be infiltrated into the gap of the tubular braid. Besides, PLA fibers were dissolved partially by NMP in casting solution during spinning process. Therefore, the separation layer gets adhered to the tubular braid to form a good interfacial bonding [38]. The separation layer presented an asymmetric structure which consists of a dense skin layer and a finger-like structure sub-layer. As the PEG molecular weight increased, the thickness of skin layer increased significantly [39]. Meanwhile, the pore number and its size decreased as the PEG molecular weight increased. It can be seen from Fig. 3 that the shear viscosity of casting solution increased with the increase of the PEG molecular weight. With the shear viscosity increasing, the double diffusion rate of solvent and non-solvent in the coagulation became lower, which delayed the phase transformation process and inhibited the formation and growth of finger-like structure [40].

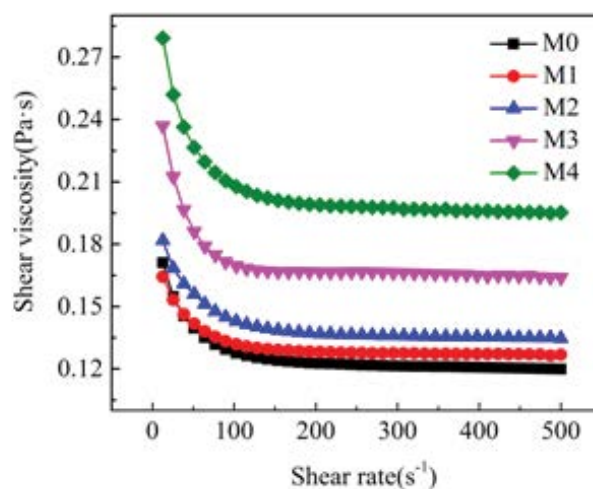


Fig. 3. Effect of PEG molecular weight on shear viscosity of casting solution (M0, M1 PEG400, M2 PEG2000, M3 PEG10000, M4 PEG20000).

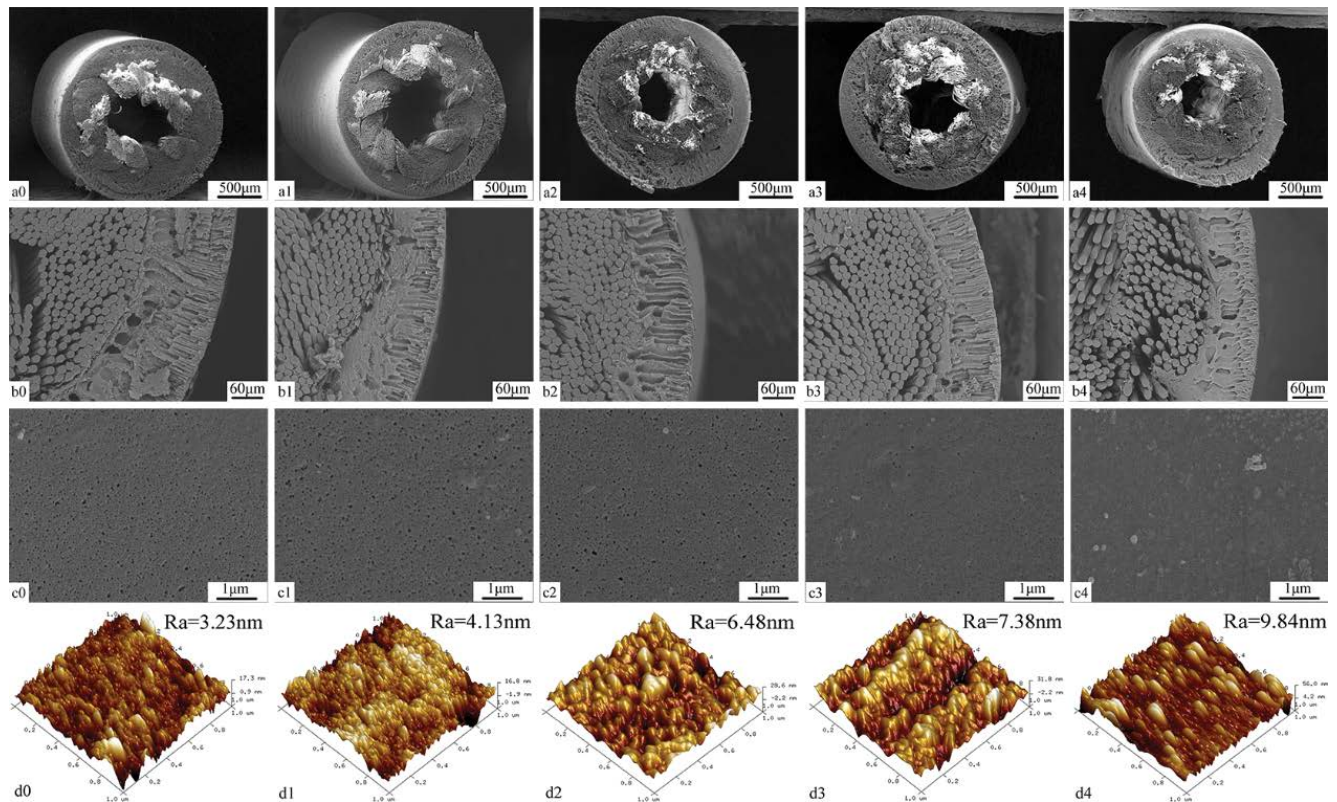


Fig. 4. SEM and AFM images of HMR PLA membranes with different PEG molecular weight: (a) cross section; (b) partial cross section; (c) outer surface; and (d) surface roughness; (0–4) M0–M4.

The AFM morphology and roughness parameters of HMR PLA membranes are also shown in Fig. 4. It could be seen clearly that the surface roughness of HMR PLA hollow fiber membranes increased with the increase of PEG molecular weight. This was mainly due to the membrane structure of HMR PLA hollow fiber membranes changing rougher with the increase of PEG molecular weight.

Table 2 shows the separation layer thickness of HMR PLA hollow fiber membranes. It was clear that the thickness of separation layer decreased with the increase of PEG molecular weight. As shown in Fig. 3, the shear viscosity of casting solution increased with the increase of the PEG molecular weight. During spinning process, the higher viscosity of casting solution, the less casting solution could be coated on membrane surface. Therefore, the thickness of separation layer decreased with the increase of PEG molecular weight. It can be seen clearly that the mean pore size decreased with the increase of PEG molecular weight, the result is consistent with Fig. 4.

Fig. 5 shows the contact angle of the HMR PLA hollow fiber membranes. As can be seen from the figure, the

water contact angle decreased with the increase of PEG molecular weight. It was difficult to wash out the PEG molecular chains from the membranes with the increase of PEG molecular weight. Meanwhile, the PEG was a hydrophilic polymer. Moreover, the surface roughness of HMR PLA hollow fiber membranes increased with the increase of PEG molecular weight. Therefore, the water contact angle showed a decreasing trend [41].

Fig. 6 shows the stress–strain curves of the PLA tubular braid and HMR (M0) PLA hollow fiber membranes. The mechanical properties of HMR PLA hollow fiber membranes were mainly provided by three aspects: tubular braid, surface layer and their interface bonding layer [42].

The tensile strength and breaking elongation of HMR (M0) were lower than that of the tubular braid due to the NMP in casting solution had a certain solubility of PLA fiber. Moreover, the initial modulus of HMR (M0) was higher than PLA tubular braid. The PLA casting solution could embed in the gaps between the fibers of tubular braid during the spinning process. Hence, the separation layer and the PLA tubular braid could combine tighter

Table 2
Separation layer thickness and mean pore size of HMR PLA hollow fiber membranes

Membrane	M0	M1	M2	M3	M4
Separation layer thickness (μm)	118.3 ± 4.8	107.3 ± 3.6	98.4 ± 4.3	94.6 ± 4.2	90.7 ± 3.4
Mean pore size (μm)	0.1716	0.1495	0.1340	0.1126	0.1040

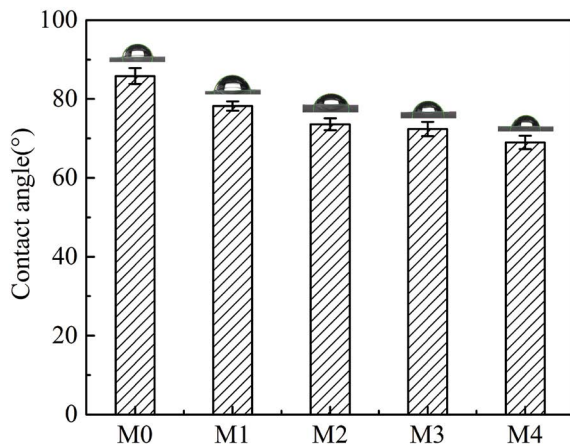


Fig. 5. Effect of PEG molecular weight on contact angle of HMR PLA hollow fiber membranes (M0, M1 PEG400, M2 PEG2000, M3 PEG10000, M4 PEG20000).

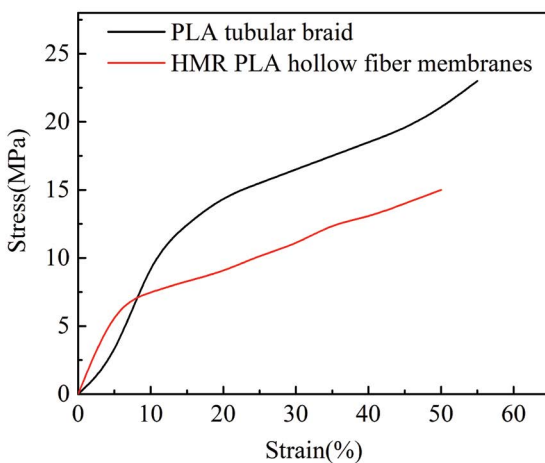
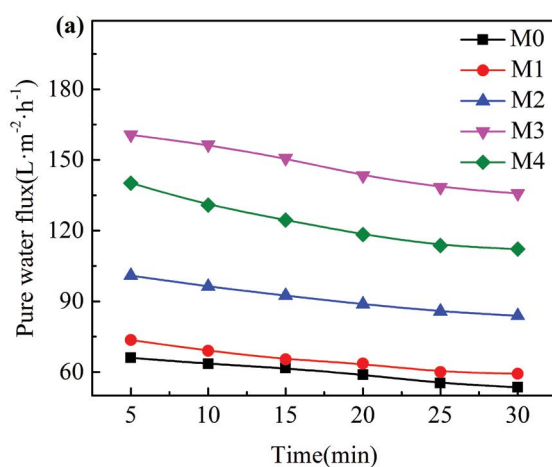


Fig. 6. Mechanical properties of HMR PLA hollow fiber membranes and the PLA tubular braid.



and hinder the deformation of the PLA tubular braid structure [43].

Fig. 7a shows the PWF of HMR PLA hollow fiber membranes. It can be seen that the PWF first increased and then decreased with the increase of PEG molecular weight. With the increase of PEG molecular weight from 400 to 10,000, the PWF increased from 59.3 to 135.8 L m⁻² h⁻¹. When the molecular weight continued to increase to 20,000, the PWF decreased to 112.2 L m⁻² h⁻¹. Although the mean pore size decreased with PEG molecular weight increased to 10,000, the increasing/higher hydrophilicity and thinner separation layer led to an increase of the PWF. When PEG molecular weight increased from 10,000 to 20,000, the thickness of separation layer decreased slightly. While the surface layer became denser, this may led to a PWF decrease of M4.

Fig. 7b shows the BSA rejection of the HMR PLA hollow fiber membranes. It can be seen clearly that with the PEG molecular weight increase, the rejection increased. This was because that the membrane structure got more compact and the surface was denser with the increase of PEG molecular weight. When the molecular weight of PEG reached 10,000, the surface of the membranes was dense enough, the BSA rejection increased slightly although the PEG molecular weight continued to increase.

Fig. 8 shows the permeate flux and FRR, DR values during the BSA solution filtration of HMR PLA hollow fiber membranes, respectively. As can be seen from Fig. 8a, when the feed solution was changed from pure water to BSA solution, the permeate flux sharply dropped due to the higher viscosity of BSA solution and protein adsorption of the membranes. Then the membranes were washed by deionized water to recover their permeability after BSA solution filtration experiment. The washing process was continued for 10 min. Finally, the PWF of the washed HMR PLA hollow fiber membranes was tested. As can be seen from Fig. 8b, the FRR of M0, M1, M2, M3 and M4 increased with the increase of PEG molecular weight, while the DR decreased. This meant that the HMR PLA hollow fiber membranes showed a better anti-fouling performance with the increase of PEG molecular weight. The smaller pore size, higher surface roughness

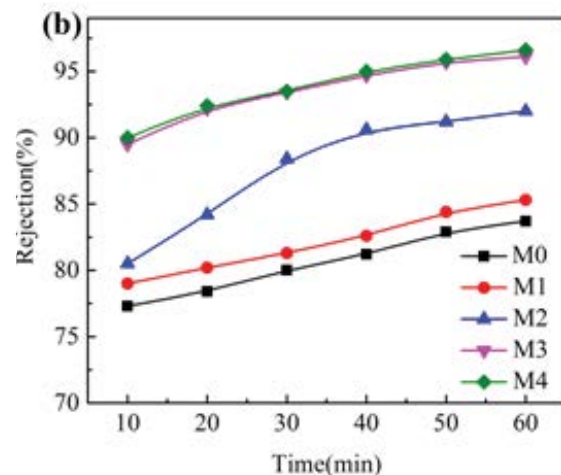


Fig. 7. Effect of PEG molecular weight on PWF (a) and BSA rejection (b) of HMR PLA hollow fiber membranes (M0, M1 PEG400, M2 PEG2000, M3 PEG10000, M4 PEG20000).

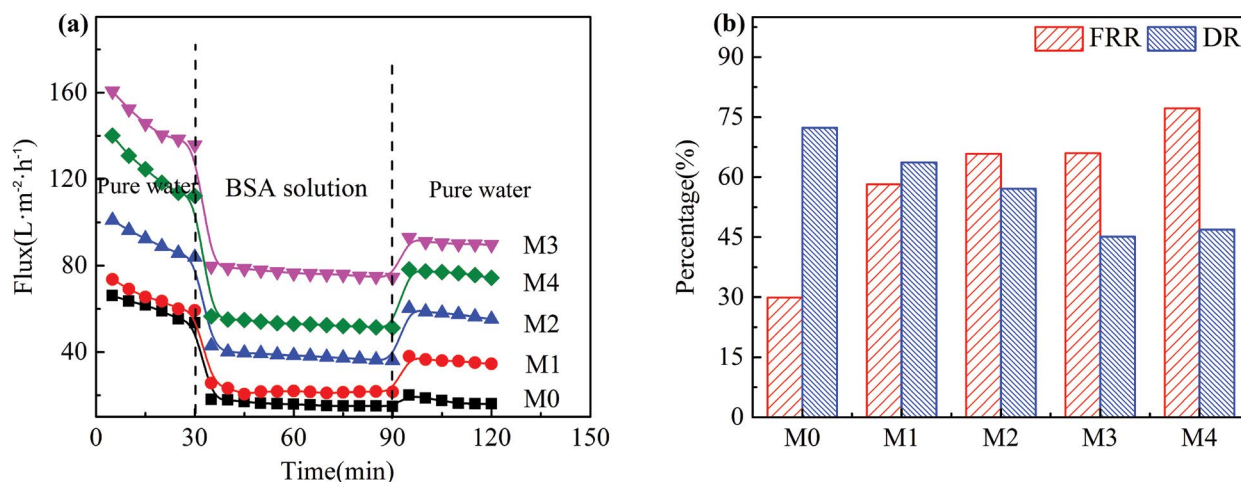


Fig. 8. Effect of PEG molecular weight on permeate flux (a) and FRR, DR values (b) of HMR PLA hollow fiber membranes during the process (M0, M1 PEG400, M2 PEG2000, M3 PEG10000, M4 PEG20000).

and higher hydrophilicity of membrane were beneficial to enhance the anti-fouling performance of HMR PLA hollow fiber membranes. As discussed above, the increase of PEG molecular weight led to a smaller pore size, higher surface roughness and higher hydrophilicity. Therefore, the HMR PLA hollow fiber membranes showed a better anti-fouling performance with the increase of PEG molecular weight.

3.2. Interfacial bonding properties of HMR and HTR PLA hollow fiber membranes

The price of PET tubular braid was cheap and mechanical property of it was superior to PLA tubular braid. Therefore, the PET tubular braid was selected as the heterogeneous tubular braid to prepare the HTR (M5) PLA hollow fiber membranes. In order to study the effect of tubular braid on interfacial bonding properties, the HMR (M3) and HTR (M5) PLA hollow fiber membranes were prepared with the same composition of the casting solution. Fig. 9 shows the SEM images of the cross section of HMR (M3) and HTR (M5) PLA hollow fiber membranes. As can be seen from the figure, the separation layer was tightly bonded with the tubular braid of HMR (M3) PLA hollow fiber membranes, while there was a poor interfacial bonding state between the separation layer and the tubular braid of HTR (M5) PLA hollow fiber membranes due to their incompatibility. For HMR (M3) PLA hollow fiber membranes, the NMP in the casting solution can dissolve the PLA fiber of the tubular braid surface. Therefore, the PLA chains in the casting solution and the PLA chains of the tubular braid surface can mutually diffuse, and solidify by the coagulation bath to form a relatively firm interfacial bonding. For HTR (M5) PLA hollow fiber membranes, there was a clear boundary between the surface separation layer and the PET tubular braid. The casting solution was less immersed in the PET tubular braid and the PET fiber cannot be swollen by the casting solution, which was not conducive to the formation of a good interfacial bonding.

Physical backwashing was the basic method for cleaning membranes in membrane separation technology, and the interfacial bonding performance was relatively important

during this process. Therefore, the interfacial bonding performance was a key factor of reinforced hollow fiber membranes. The bursting strength was determined by the separation layer and the interfacial bonding performance. And the separation layer of HMR (M3) and HTR (M5) was prepared under the same conditions, hence the bursting strength of HMR (M3) and HTR (M5) was determined by the interfacial bonding performance of them. The interfacial bonding state of HMR (M3) and HTR (M5) will be broken during the backwashing process if the operating pressure was too high. Therefore, the bursting strength can be tested by backwashing process. The HMR (M3) and HTR (M5) were backwashed for 12 h at 0.1 MPa. The separation layer of HMR (M3) and HTR (M5) was not damaged or peeled off. This indicated that both of them can be used at low pressure. When the pressurization rate was 0.001 MPa min⁻¹, the separation layer of HTR (M5) broken at 0.250 MPa, and the separation layer of HMR (M3) broken at 0.600 MPa. The result indicated that the interfacial bonding state of HMR (M3) was better than that of HTR (M5).

Ultrasonic energy can be used to clean objects, destroy bacterial structures and disinfect objects, so this method can be used for cleaning the membranes and characterize the interfacial bonding state of the reinforced hollow fiber membranes [44]. Fig. 10 shows the pore size distribution of the HMR (M3) and HTR (M5) before and after the ultrasonic water bath oscillation. It can be seen that the average pore size of HMR (M3) and HTR (M5) was all increased after sonication. The pore size distribution of HMR (M3) was almost unchanged, while the pore size distribution of HTR (M5) was broadened. For HMR (M3), the separation layer and the tubular braid were the same material. As described above, the solvent NMP had a certain dissolution on the PLA tubular braid, which led to a relatively firm interfacial bonding. After solidified by the coagulation bath, the pore diameter changed a little due to the minor damage of the interfacial bonding state which caused by the ultrasonic oscillation. For HTR (M5), the pore structure significantly changed due to its poor interfacial bonding state. The ultrasonic oscillation caused partial damage to the interface or even caused the

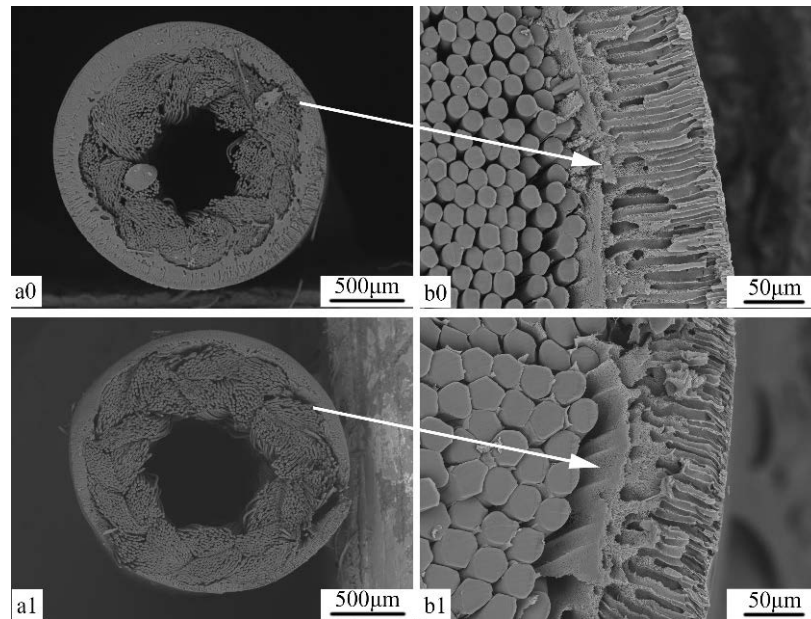


Fig. 9. SEM images of PLA hollow fiber membranes: (a0) cross section of HMR (M3); (b0) partial cross section of HMR (M3); (a1) cross section of HTR (M5); and (b1) partial cross section of HMR (M5).

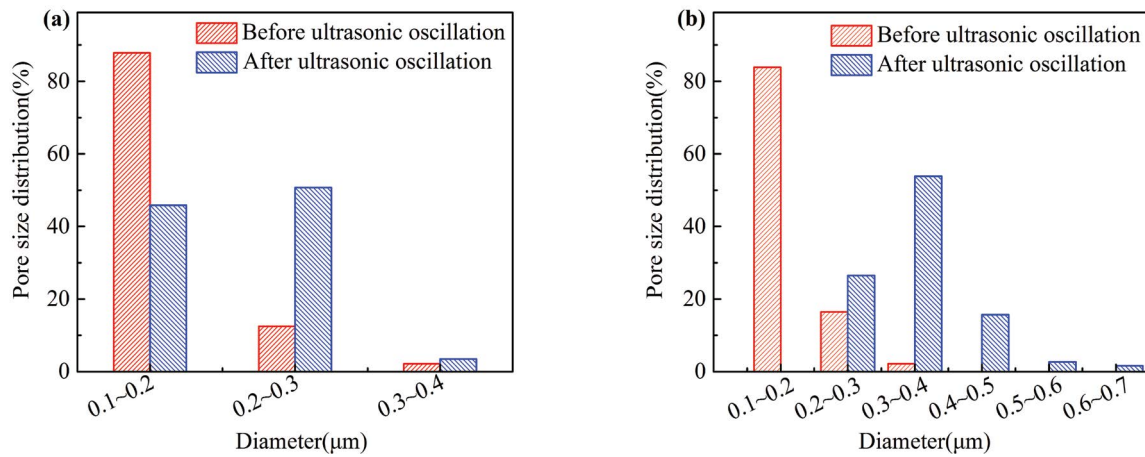


Fig. 10. Effect of ultrasonic water bath oscillation on the pore size distribution of HMR (M3) (a) and HTR (M5) (b).

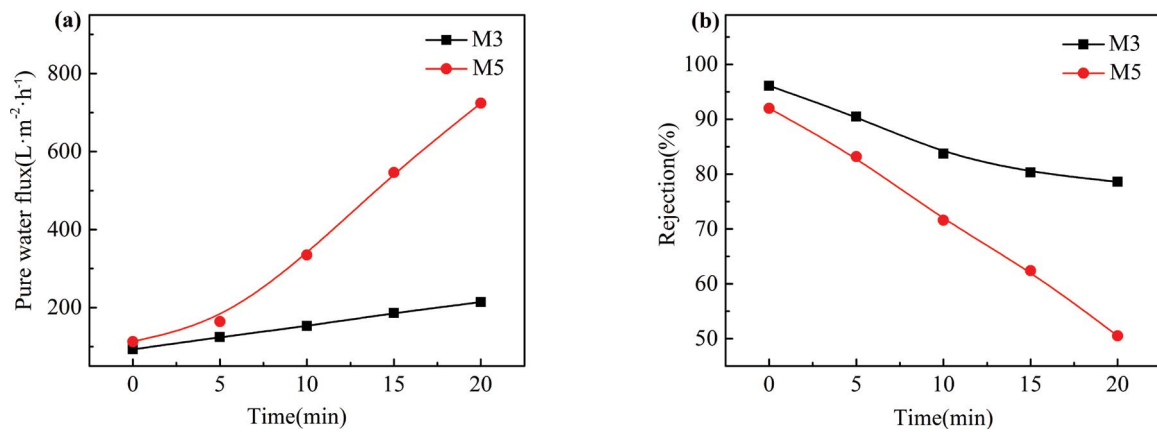


Fig. 11. Effect of ultrasonic water bath oscillation on the PWF (a) and BSA rejection (b) of HMR (M3) and HMR (M5).

separation layer to peel off from the tubular braid. Therefore, the pore size distribution of HTR (M5) became wider and the number of large pores remarkably increased.

Fig. 11 shows the PWF and BSA rejection of the HMR (M3) and HTR (M5) after ultrasonic water bath oscillation. It can be seen that the PWF and BSA rejection were all changed with the increase of ultrasonic time, while the variation of HTR (M5) was obviously higher than HMR (M3). The high energy of the ultrasonic wave caused the damage of interfacial bonding state and pore structure of BR PLA hollow fiber membranes, which led to an increase of water flux and a reduction of BSA rejection. The ultrasonic had a little effect on the interfacial bonding state and the pore structure of HMR (M3) than that of HTR (M5) due to the interfacial bonding of HMR (M3) was superior to that of HTR (M5). Therefore, the PWF and BSA rejection variation of HMR (M3) were lower than that of HTR (M5). This further demonstrated the superior interfacial bonding performance of HMR (M3) than that of HTR (M5).

4. Conclusion

In this paper, the BR PLA hollow fiber membranes were prepared by concentric circular spinning technology. The effect of PEG molecular weight on membranes structure and properties was studied. The interfacial bonding state of HMR and HTR PLA hollow fiber membranes was also discussed. The PWF and BSA rejection increased with the increase of PEG molecular weight from 400 to 10,000. When the PEG molecular weight continued to increase, the PWF decreased and the BSA rejection increased a little. The anti-fouling performance of the membranes increased with the increase of PEG molecular weight due to the increased surface roughness and hydrophilicity. In addition, the interfacial bonding properties of the HMR PLA hollow fiber membranes were better than the HTR PLA hollow fiber membranes due to the incompatibility of PET tubular braid and the casting solution of HTR PLA hollow fiber membranes. In conclusion, the optimum PEG molecular weight was 10,000, the water flux was $135.8 \text{ L m}^{-2} \text{ h}^{-1}$ and the BSA rejection was 96.1 %, the PLA tubular braid was a better matrix to prepare BR PLA hollow fiber membranes.

Acknowledgements

The authors thank the financial support of the National Natural Science Foundation of China (NFSC, 51673149).

References

- [1] S.S. Yoo, I. Choi, S.M. Ji, K.B. Ko, K.H. Chu, Operating cost reduction of UF membrane filtration process for drinking water treatment attributed to chemical cleaning optimization, *J. Environ. Manage.*, 206 (2018) 1126–1134.
- [2] C.M. Chew, M.K. Aroua, M.A. Hussain, Advanced process control for ultrafiltration membrane water treatment system, *J. Cleaner Prod.*, 179 (2018) 63–80.
- [3] S.I. Patsios, A.J. Karabelas, An investigation of the long-term filtration performance of a membrane bioreactor (MBR): the role of specific organic fractions, *J. Membr. Sci.*, 372 (2011) 102–115.
- [4] H.-H. Chang, L.-K. Chang, C.-D. Yang, D.-J. Lin, L.-P. Cheng, Effect of polar rotation on the formation of porous poly(vinylidene fluoride) membranes by immersion precipitation in an alcohol bath, *J. Membr. Sci.*, 513 (2016) 186–196.
- [5] M.-m. Tao, F. Liu, B.-r. Ma, L.-x. Xue, Effect of solvent power on PVDF membrane polymorphism during phase inversion, *Desalination*, 316 (2013) 137–145.
- [6] S.M. Mousavi, A. Zadhoush, Investigation of the relation between viscoelastic properties of polysulfone solutions, phase inversion process and membrane morphology: the effect of solvent power, *J. Membr. Sci.*, 532 (2017) 47–57.
- [7] M. Mailvaganam, L. Fabbriano, C.F.F. Rodrigues, A.R. Donnelly, Hollow fiber semipermeable membrane of tubular braid, US5472607, 1995-12-05.
- [8] M.-S. Lee, S.-H. Choi, Y.-C. Shin, Braid-reinforced hollow fiber membrane, US7267872B2, 2007-09-11.
- [9] X. Zhang, C. Xiao, X. Hu, Q. Bai, Preparation and properties of homogeneous-reinforced polyvinylidene fluoride hollow fiber membrane, *Appl. Surf. Sci.*, 264 (2013) 801–810.
- [10] M.J. Kim, B. Sankararao, C.K. Yoo, Determination of MBR fouling and chemical cleaning interval using statistical methods applied on dynamic index data, *J. Membr. Sci.*, 375 (2011) 345–353.
- [11] H. Liu, C. Xiao, Q. Huang, X. Hu, Structure design and performance study on homogeneous-reinforced polyvinyl chloride hollow fiber membranes, *Desalination*, 331 (2013) 35–45.
- [12] H. Liu, C. Xiao, Q. Huang, X. Hu, W. Shu, Preparation and interface structure study on dual-layer polyvinyl chloride matrix reinforced hollow fiber membranes, *J. Membr. Sci.*, 472 (2014) 210–221.
- [13] Z. Fan, C. Xiao, H. Liu, Q. Huang, J. Zhao, Structure design and performance study on braid-reinforced cellulose acetate hollow fiber membranes, *J. Membr. Sci.*, 486 (2015) 248–256.
- [14] H. Wu, Y. Liu, L. Mao, C. Jiang, J. Ang, X. Lu, Doping polysulfone ultrafiltration membrane with TiO_2 -PDA nanohybrid for simultaneous self-cleaning and self-protection, *J. Membr. Sci.*, 532 (2017) 20–29.
- [15] C. Yang, H. Tong, C. Luo, S. Yuan, G. Chen, Y. Yang, Boehmite particle coating modified microporous polyethylene membrane: a promising separator for lithium ion batteries, *J. Power Sources*, 348 (2017) 80–86.
- [16] S. Roualdes, N. Kourda, J. Durand, G. Pourcelly, Plasma-grafted PVDF polymers as anion exchange membranes for the electrotransport of Cr(VI), *Desalination*, 146 (2018) 273–278.
- [17] Z.M. Liu, Z.K. Xu, J.Q. Wang, Q. Yang, J. Wu, P. Seta, Surface modification of microporous polypropylene membranes by the grafting of poly(γ -stearyl-l-glutamate), *Eur. Polym. J.*, 39 (2003) 2291–2299.
- [18] H. Zhang, M. Liu, D. Sun, B. Li, P. Li, Evaluation of commercial PTFE membranes for desalination of brine water through vacuum membrane distillation, *Chem. Eng. Process.*, 110 (2016) 52–63.
- [19] F. Galiano, K. Briceño, T. Marino, A. Molino, K.V. Christensen, A. Figoli, Advances in biopolymer-based membrane preparation and applications, *J. Membr. Sci.*, 564 (2018) 562–586.
- [20] C. Delabarde, C.J.G. Plummer, J.A.E. Manson, Biodegradable polylactide/hydroxyapatite nanocomposite foam scaffolds for bone tissue engineering applications, *J. Mater. Sci. - Mater. Med.*, 23 (2012) 1371–1385.
- [21] R.E. Drumright, P.R. Gruber, D.E. Henton, Poly(lactic acid) technology, *Adv. Mater.*, 12 (2000) 1841–1846.
- [22] A. Marra, C. Silvestre, D. Duraccio, S. Cimmino, Poly(lactic acid)/zinc oxide biocomposite films for food packaging application, *Int. J. Biol. Macromol.*, 88 (2016) 254–262.
- [23] S. Kumar, S. Singh, S. Senapati, A.P. Singh, B. Ray, P. Maiti, Controlled drug release through regulated biodegradation of poly(lactic acid) using inorganic salts, *Int. J. Biol. Macromol.*, 104 (2017) 487–497.
- [24] V. Nagarajan, A.K. Mohanty, M. Misra, Perspective on poly(lactic acid) (PLA) based sustainable materials for durable applications: focus on toughness and heat resistance, *ACS Sustainable Chem. Eng.*, 4 (2016) 2899–2916.
- [25] A. Moriya, P. Shen, Y. Ohmukai, T. Maruyama, H. Matsuyama, Reduction of fouling on poly(lactic acid) hollow fiber membranes by blending with poly(lactic acid)-polyethylene

- glycol–poly(lactic acid) triblock copolymers, *J. Membr. Sci.* 415–416 (2012) 712–717.
- [26] H. Minbu, A. Ochiai, T. Kawase, M. Taniguchi, D.R. Lloyd, T. Tanaka, Preparation of poly(L-lactic acid) microfiltration membranes by a nonsolvent-induced phase separation method with the aid of surfactants, *J. Membr. Sci.*, 479 (2015) 85–94.
- [27] F.H.H. Abdellatif, J. Babin, C. Arnal-Herault, C. Nouvel, J.-L. Six, A. Jonquieres, Bio-based membranes for ethyl tert-butyl ether (ETBE) bio-fuel purification by pervaporation, *J. Membr. Sci.*, 524 (2017) 449–459.
- [28] S. Zereshki, A. Figoli, S.S. Madaeni, S. Simone, J.C. Jansen, M. Esmailinezhad, E. Drioli, Poly(lactic acid)/poly(vinyl pyrrolidone) blend membranes: Effect of membrane composition on pervaporation separation of ethanol/cyclohexane mixture, *J. Membr. Sci.*, 362 (2010) 105–112.
- [29] T. Komatsuka, K. Nagai, Temperature dependence on gas permeability and permselectivity of poly(lactic acid) blend membranes, *Polym. J.*, 41 (2009) 455–458.
- [30] A. Iulianelli, C. Algieri, L. Donato, A. Garofalo, F. Galiano, G. Bagnato, A. Basile, A. Figoli, New PEEK-WC and PLA membranes for H₂ separation, *Int. J. Hydrogen Energy*, 42 (2017) 22138–22148.
- [31] J.E. Mark, *Polymer Data Handbook*, Oxford University Press, 1999.
- [32] V. La Carrubba, F.C. Pavia, V. Brucato, S. Piccarolo, PLLA/PLA scaffolds prepared via thermally induced phase separation (TIPS): tuning of properties and biodegradability, *Int. J. Mater. Form.*, 1 (2008) 619–622.
- [33] R. Hu, Y. Pi, N. Wang, Q. Zhang, J. Feng, W. Xu, X. Dong, D. Wang, H. Yang, The formation of the S-shaped edge-on lamellae on the thin porous polylactic acid membrane via phase separation induced by water microdroplets, *J. Appl. Polym. Sci.*, 133 (2016) 6.
- [34] T. Tanaka, D.R. Lloyd, Formation of poly(L-lactic acid) micro-filtration membranes via thermally induced phase separation, *J. Membr. Sci.*, 238 (2004) 65–73.
- [35] S. Chen, Z. He, G. Xu, X. Xiao, Fabrication and characterization of modified nanofibrous poly(L-lactic acid) scaffolds by thermally induced phase separation technique and aminolysis for promoting cytocompatibility, *J. Biomater. Sci., Polym. Ed.*, 27 (2016) 1058–1068.
- [36] W.-L. Chou, D.-G. Yu, M.-C. Yang, C.-H. Jou, Effect of molecular weight and concentration of PEG additives on morphology and permeation performance of cellulose acetate hollow fibers, *Sep. Purif. Technol.*, 57 (2007) 209–219.
- [37] E. Saljoughi, M. Amirilargani, T. Mohammadi, Effect of PEG additive and coagulation bath temperature on the morphology, permeability and thermal/chemical stability of asymmetric CA membranes, *Desalination*, 262 (2010) 72–78.
- [38] Z. Fan, C. Xiao, H. Liu, Q. Huang, Preparation and performance of homogeneous braid reinforced cellulose acetate hollow fiber membranes, *Cellulose*, 22 (2015) 695–707.
- [39] A. Gao, F. Liu, H. Shi, L. Xue, Controllable transition from finger-like pores to inter-connected pores of PLLA membranes, *J. Membr. Sci.*, 478 (2015) 96–104.
- [40] S.H. Yoo, J.H. Kim, J.Y. Jho, J. Won, S.K. Yong, Influence of the addition of PVP on the morphology of asymmetric polyimide phase inversion membranes: effect of PVP molecular weight, *J. Membr. Sci.*, 236 (2004) 203–207.
- [41] B. Chakrabarty, A.K. Ghoshal, M.K. Purkait, Effect of molecular weight of PEG on membrane morphology and transport properties, *J. Membr. Sci.*, 309 (2008) 209–221.
- [42] Q. Quan, C. Xiao, H. Liu, Q. Huang, W. Zhao, X. Hu, G. Huan, Preparation and characterization of braided tube reinforced polyacrylonitrile hollow fiber membranes, *J. Appl. Polym. Sci.*, 132 (2015) 14.
- [43] M. Chen, C. Xiao, C. Wang, H. Liu, Study on the structural design and performance of novel braid-reinforced and thermostable poly(*m*-phenylene isophthalamide) hollow fiber membranes, *RSC Adv.*, 7 (2017) 20327–20335.
- [44] I. Masselin, X. Chasseray, L. Durand-Bourlier, J.-M. Lainé, P.-Y. Syzaret, D. Lemordant, Effect of sonication on polymeric membranes, *J. Membr. Sci.*, 181 (2001) 213–220.